# The Retinoblastoma Binding Protein RBP2 Is an H3K4 Demethylase

Robert J. Klose,[1,2,6] Qin Yan,[1,3,6] Zuzana Tothova,[1,4] Kenichi Yamane,[1,2] Hediye Erdjument-Bromage,[5] Paul Tempst,[5] D. Gary Gilliland,[1,4] Yi Zhang,[1,2,*] and William G. Kaelin, Jr.[1,3,*]
[1] Howard Hughes Medical Institute
[2] Department of Biochemistry and Biophysics, Lineberger Comprehensive Cancer Center
University of North Carolina at Chapel Hill, Chapel Hill, NC 27599, USA
[3] Department of Medical Oncology, Dana-Farber Cancer Institute, and Brigham and Women's Hospital
[4] Division of Hematology, Department of Medicine, Brigham and Women's Hospital
Harvard Medical School, Boston, MA 02115, USA
[5] Molecular Biology Program, Memorial Sloan Kettering Cancer Center, 1275 York Avenue, New York, NY 10021, USA
[6] These authors contributed equally to this work.
*Correspondence: yi_zhang@med.unc.edu (Y.Z.), william_kaelin@dfci.harvard.edu (W.G.K.)
DOI 10.1016/j.cell.2007.02.013

## SUMMARY

Changes in histone methylation status regulate chromatin structure and DNA-dependent processes such as transcription. Recent studies indicate that, analogous to other histone modifications, histone methylation is reversible. Retinoblastoma binding protein 2 (RBP2), a nuclear protein implicated in the regulation of transcription and differentiation by the retinoblastoma tumor suppressor protein, contains a JmjC domain recently defined as a histone demethylase signature motif. Here we report that RBP2 is a demethylase that specifically catalyzes demethylation on H3K4, whose methylation is normally associated with transcriptionally active genes. *RBP2−/−* mouse cells displayed enhanced transcription of certain cytokine genes, which, in the case of *SDF1,* was associated with increased H3K4 trimethylation. Furthermore, RBP2 specifically demethylated H3K4 in biochemical and cell-based assays. These studies provide mechanistic insights into transcriptional regulation by RBP2 and provide the first example of a mammalian enzyme capable of erasing trimethylated H3K4.

## INTRODUCTION

Histones are subject to a variety of posttranslational modifications that affect chromatin structure and therefore influence processes such as transcription and DNA repair. These modifications include acetylation, methylation, phosphorylation, sumoylation, and ubiquitylation (reviewed in Shilatifard, 2006).

Recent studies have highlighted the importance of histone methylation on specific lysine residues with respect to gene regulation. Three families of enzymes are capable of mediating histone-lysyl methylation: the PRMT1 family, the SET-domain-containing protein family, and the non-SET-domain proteins DOT1 and DOT1L (reviewed in Martin and Zhang, 2005). Specific histone-lysyl residues can become mono- (me1), di- (me2), or trimethylated (me3). Whether methylation leads to transcriptional activation or repression is influenced by a variety of factors, including the histone (for example, H3 versus H4), the lysine acceptor (for example, H3K4 versus H3K9), the histone location (for example, whether bound to a coding versus noncoding region of a gene), and other contextual influences. In general, methylation on H3K9, H3K27, or H4K20 is linked to formation of tightly packed chromatin (heterochromatin) and gene silencing while methylation on H3K4, H3K36, and H3K79 is associated with actively transcribed regions (euchromatin) (Martin and Zhang, 2005). The effect of histone methylation on chromatin structure is probably not direct but, rather, through the recruitment of proteins that recognize and bind to methylated lysine. To date, four protein subdomains that are capable of binding to methylated lysine have been identified: the chromodomain (Bannister et al., 2001; Fischle et al., 2003; Lachner et al., 2001; Min et al., 2003; Pray-Grant et al., 2005), the tudor domain (Huang et al., 2006; Huyen et al., 2004; Sanders et al., 2004), the WD40 repeat (Wysocka et al., 2005), and the plant homeodomain (PHD) (Li et al., 2006; Pena et al., 2006; Shi et al., 2006; Wysocka et al., 2006).

Histone-lysyl methylation, like histone acetylation, is reversible. The first lysyl demethylase to be identified was lysine-specific demethylase 1 (LSD1), which demethylates H3K4 or H3K9 in a reaction that utilizes flavin as a cofactor and which is limited to mono- or dimethylated substrates (Shi et al., 2004). In 2005 Trewick and coworkers predicted the existence of a second class of histone demethylases that contain a JmjC domain (Trewick et al., 2005), which

is a motif present in many proteins that are known, or suspected, to play roles in transcription. They noted that the JmjC domain of the yeast protein Epe1 could be modeled onto the JmjC domain of the FIH1 protein hydroxylase, which utilizes iron and 2-oxoglutarate as cofactors to hydroxylate HIF. Moreover, FIH1 residues necessary for binding to iron and 2-oxoglutarate appeared to be conserved in at least a subset of JmjC domains. They speculated that some JmjC proteins might hydroxylate methylated lysine residues, which would then spontaneously undergo conversion to unmethylated lysine with release of formaldehyde. This hypothesis was informed by the earlier observation that the 2-oxoglutarate and iron-dependent hydroxylase AlkB demethylates damaged DNA in an analogous reaction (Falnes et al., 2002; Trewick et al., 2002).

Zhang and coworkers independently came to these same conjectures and successfully isolated the JmjC domain protein JHDM1 upon purifying a histone H3K36 demethylase activity from cells, using formaldehyde release as their readout (Tsukada et al., 2006). Since that time, several other JmjC-domain-containing proteins have been shown to possess histone demethylase activity toward specific histone methylation marks (Cloos et al., 2006; Fodor et al., 2006; Klose et al., 2006b; Whetstine et al., 2006; Yamane et al., 2006). Thirty JmjC-domain-containing proteins have been identified in humans, which can be phylogenetically divided into seven subfamilies (JHDM1, JHDM2, PHF2/PHF8, JARID, JHDM3/JMJD2, UTX/UTY, and JmjC-domain-only family) (Klose et al., 2006a). So far only members of the JHDM1, JHDM2, and JHDM3/JMJD2 families have been shown to possess histone demethylase activity (Klose et al., 2006a). It is unlikely that all of the human JmjC-domain proteins are demethylases since some have nonconservative substitutions at residues that are predicted to be important for coordinating iron and 2-oxoglutarate.

RBP2 is a nuclear phosphoprotein that was initially identified as a potential pRB binding protein (Defeo-Jones et al., 1991). Native chromatin-associated pRB-RBP2 complexes are detected in response to signals that affect cell-cycle exit and induction of differentiation (Benevolenskaya et al., 2005). RBP2 is encoded by one of the four paralogous JARID-family genes in humans (Kortschak et al., 2000; Wilsker et al., 2005) and, in addition to a JmjC domain, contains other domains that are frequently found in transcriptional regulators, including a JmjN domain, a Bright/Arid domain, a C5H2C zinc finger, and several PHD domains. The *Drosophila RBP2* ortholog, *Lid*, was originally identified in a screen for novel Trithorax member genes (Gildea et al., 2000), which also implies a potential role for RBP2 in transcriptional regulation. It appears that free RBP2 can repress certain genes involved in differentiation and that binding to pRB converts RBP2 from a transcriptional repressor to a transcriptional activator (Benevolenskaya et al., 2005). How, mechanistically, RBP2 regulates transcription is not known.

## RESULTS

### RBP2 Is a Histone Demethylase

The JmjC domain of JARID1 proteins share extensive similarity to the JmjC domain of the JHDM3 demethylases, which target removal of H3K9/36 methylation and can remove the trimethyl modification state (Figure 1A). Conservation of residues within the predicted cofactor binding sites of the RBP2 JmjC domain and the apparent role of RBP2 as a transcriptional regulator led us to ask if RBP2 possessed histone demethylase activity and, if so, whether this activity might be directed toward a histone methylation mark that was not recognized by the previously characterized JmjC-family members.

In pilot experiments we discovered that partially purified RBP2 from mammalian cell extracts could specifically demethylate trimethylated H3K4, suggesting that RBP2, or perhaps an associated protein, was responsible for this activity (data not shown).

Currently, LSD1 is the only characterized H3K4 demethylase, but its catalytic requirement for a protonated nitrogen on the lysine-amine group limits its enzymatic activity to H3K4me1/me2 modified substrates (Lee et al., 2005; Metzger et al., 2005; Shi et al., 2004, 2005). The inability of LSD1 to reverse H3K4me3 left open the possibility that this modification state is refractory to enzymatic demethylation. In contrast to LSD1, the JmjC-domain-containing histone demethylases exploit a direct hydroxylation reaction to remove histone methylation, suggesting that RBP2 might catalyze the removal of H3K4me3.

To verify that RBP2 is an H3K4 demethylase and to examine the modification-state specificity of RBP2, Flag-tagged RBP2 was expressed in SF9 cells using a baculovirus expression system and affinity purified to homogeneity. Purified Flag-RBP2 resolved as a single band following SDS-PAGE and Coomassie blue or silver staining (Figure 1B). Recombinant RBP2 was then incubated with radioactively labeled histone substrates and demethylase activity analyzed by formaldehyde release. Recombinant RBP2 only caused release of radioactive formaldehyde when H3K4-methylated substrates were used indicating that recombinant RBP2 is an H3K4 demethylase (Figure 1C). To probe the modification-state specificity of RBP2, recombinant RBP2 was incubated in a histone demethylase assay with modified histone H3 peptide substrates corresponding to the H3K4 me3, me2, and me1 modification states (Figures 1D–1F). RBP2 displayed robust H3K4 demethylase activity against H3K4me3 and me2 (Figures 1D and 1E), resulting in 80%–90% demethylation of the modified substrate (Figures 1G and 1H), but failed to catalyze removal of the me1 modification state (Figure 1F). Although RBP2 fails to initiate demethylation of H3K4me1 in vitro (Figure 1F), it is capable of processively demethylating the H3K4me3 and me2 modifications to the unmodified state (Figures 1D and 1E). This enzymatic property of RBP2 is similar to the other trimethyl demethylase, JHDM3A, which also catalyzes processive removal of all three modification states but fails to initiate
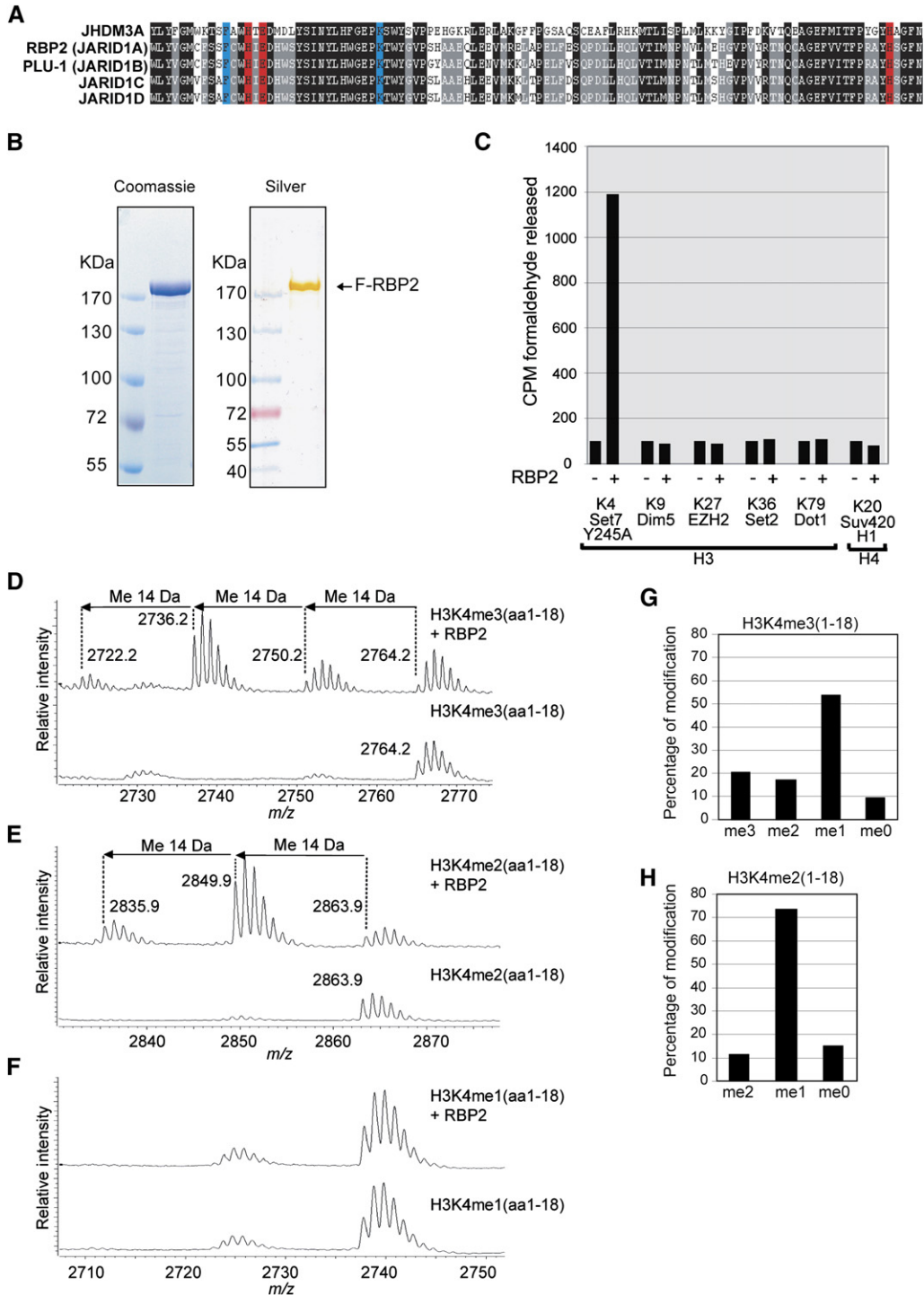
**Figure 1. RBP2 Is an H3K4 Demethylase**

(A) The JmjC domain of the JARID1 subfamily is highly similar to the JmjC domain of JHDM3 demethylase enzymes. The predicted Fe(II) (red shading) and αKG binding (blue shading) residues are conserved in RBP2 and other JARID1 members.

(B) Recombinant Flag-RBP2 was expressed in insect cells, affinity purified by Flag chromatography, and analyzed by SDS-PAGE followed by Coomassie blue or silver staining.

(C) Recombinant Flag-RBP2 was incubated with labeled histone substrates and demethylase activity monitored by formaldehyde release. RBP2 demethylates H3K4-methylated substrate.

(D–F) Mass-spectrometry analysis of RBP2 activity toward H3K4me3 (D), H3K4me2 (E), and H3K4me1 (F) peptides.

(G–H) Quantification of demethylation levels observed for RBP2 on H3K4me3 (G) and H3K4me2 (H) substrates.

demethylation on the me1 modification state in vitro (R.J.K. and Y.Z., unpublished observations). Together, these observations indicate that the H3K4me3 modification state is enzymatically reversible and suggests that histone demethylation contributes to transcriptional regulation by RBP2.

## RBP2 Demethylates H3K4 In Vivo

To ask whether RBP2 functions as an active H3K4 demethylase in vivo, a Flag-tagged RBP2 expression plasmid was transfected into NIH3T3 cells, and its effect on H3K4 methylation was analyzed by indirect immunofluorescence using H3K4 methylation specific antibodies (Figure 2). Cells overexpressing RBP2 showed a uniform reduction of H3K4me1, me2, and me3 modifications (Figures 2A–2C, top panels). Removal of H3K4 methylation was dependent on the demethylase activity of RBP2 as a point mutation in the predicted JmjC-domain iron binding site (H483A) abrogated the H3K4 demethylation (Figures 2A–2C, bottom panels). Surprisingly, given the inability of recombinant RBP2 to demethylate the H3K4me1 in vitro, RBP2 efficiently catalyzed removal of the H3K4me1 in vivo. This observation suggests that capacity of the RBP2 to catalyze H3K4me1-specific demethylation is regulated by additional factors or modifications specific to mammalian RBP2 in vivo. Collectively, these data indicate that RBP2 is able to demethylate all the H3K4 methylation states in vivo and demonstrate the H3K4me3 is a readily reversible histone modification.

## Generation of RBP2−/− Mice

Cell-culture experiments suggest that RBP2 plays a role in differentiation control by the retinoblastoma tumor suppressor protein (pRB). To begin to study the functions of RBP2 in vivo, and its genetic interactions with RB1, we set out to make RBP2−/− mice. Toward this end we made a gene-targeting vector in which RBP2 exons 5 and 6 were flanked by LoxP sites (Figure 3A). For positive and negative selection purposes this vector also contained a Neomycin resistance cassette, which was flanked by Frt sites, and a Diptheria toxin cassette, respectively. The elimination of exons 5 and 6 removes sequences that encode a portion of the RBP2 Bright/Arid domain and changes the RBP2 reading frame 3′ of the exon 4-exon 7 junction, leading to loss of the JmjC, zinc finger, and PHD domains.

The gene-targeting vector was introduced into 129/SvEv embryonic stem cells by electroporation followed by selection with G418. Cells that had undergone successful homologous recombination, as determined by PCR and Southern blot analysis, were injected into C57BL/6 blastocysts. High-percentage chimeras were backcrossed to C57BL/6 mice, which were sequentially bred to CAGG-Flpe mice, to remove the Neomycin resistance cassette, and to EIIa-Cre mice to generate the null RBP2 allele. Once germline transmission of the null RBP2 allele was confirmed RBP2+/− males were mated with RBP2+/− females. Viable RBP2−/− offspring were
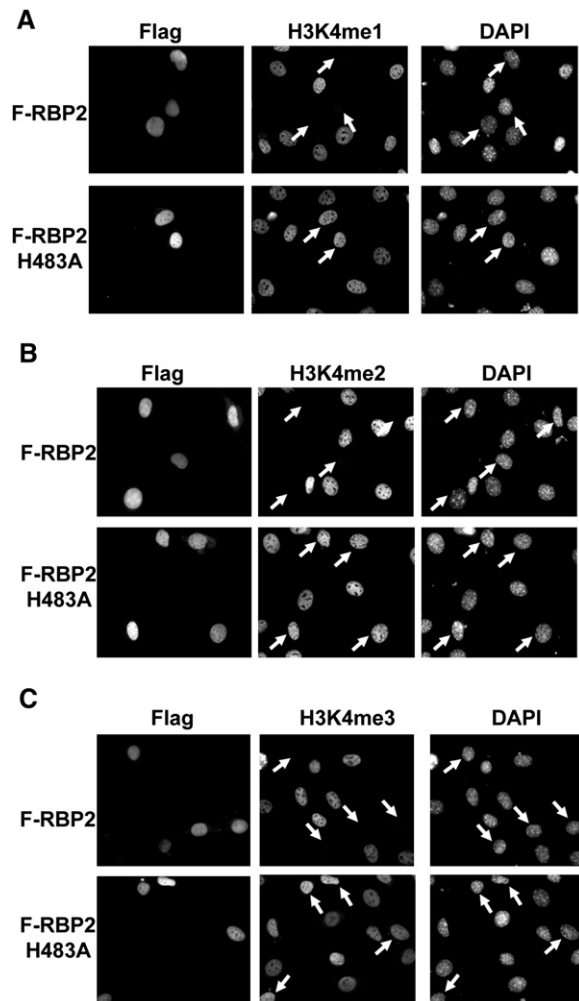


**Figure 2. RBP2 Demethylates H3K4 In Vivo**
(A–C) Flag-RBP2 or Flag-RBP2 containing a mutation in the proposed iron binding site (H483A) was expressed in NIH3T3 cells. The levels of H3K4 methylation were analyzed using modification-specific antibodies against (A) H3K4me1, (B) H3K4me2, and (C) H3K4me3 by indirect immunofluorescence (middle panels). Cells expressing wild-type and mutant RBP2 were identified by Flag immunofluoresence (left panels), and nuclei were identified by DAPI staining (right panels). Arrowheads in the middle and right panels indicate transfected cells. RBP2 demethylates all three H3K4 methylation states in vivo.

produced at the expected Mendelian frequency, and their survival does not appear to be compromised during the first nine months of life, the observation period available to date (Figures 3B and 3C, Table S1, and data not shown). As expected full-length RBP2 mRNA and protein were undetectable in RBP2−/− MEFs (Figures 3D and 3E). By real-time RT-PCR analysis we detected a weak signal using mRNA isolated from RBP2−/− MEFs and primers specific for RBP2 exons 1–3, presumably because the altered RBP2 mRNA is highly unstable (Figure 3D).

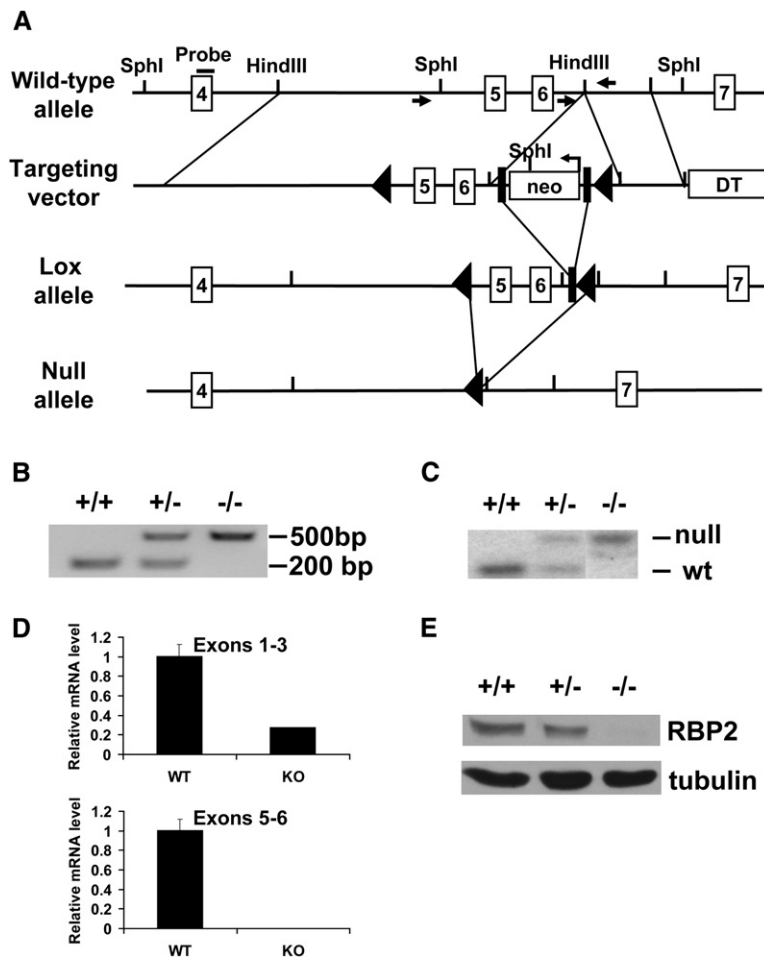RBP2−/− mice exhibited characteristic behavioral abnormalities when held upside down by the tail but

**A**



**B**



**C**



**D**



**E**



**Figure 3. Generation of *RBP2*−/− Mice**
(A) Schematic of RBP2 genomic locus and recombinant alleles. Exons are depicted by the open boxes with exon number inside. *Frt* and *LoxP* sites are indicated by filled rectangles and triangles, respectively.
(B) Multiplex PCR using primers indicated in (A) (arrows) and genomic DNA extracted from mouse tails.
(C) Southern blot analysis of genomic DNA, isolated from mouse tails, after digestion with SphI and hybridization with 5′ probe shown in (A).
(D) Quantitative, real-time RT-PCR analysis of total RNA from *RBP2*+/+ (WT) and *RBP2*−/− (KO) MEFs using primers specific for exons 1–3 (top panel) or exons 5 and 6 (bottom panel). Data were normalized to GAPDH mRNA abundance and are represented as mean ± standard deviation (SD).
(E) Western blot analysis of MEFs with the indicated genotypes.

otherwise appear to be grossly normal (data not shown). Analysis of the peripheral blood of 6-week- or 23-week-old *RBP2*−/− animals showed a relative (44% versus 58% for wild-type versus *RBP2*−/− mice, respectively) and absolute neutrophilia compared to littermate controls. This prompted a detailed analysis of the hematopoietic stem cell (HSC) and myeloid progenitor compartments by high-speed multiparameter flow cytometry. There was not a significant difference in the number of LSK (Lin⁻ Sca-1⁺ c-kit⁺) cells that contain both long-term and short-term HSC, nor were there statistically significant quantitative changes in the myeloid progenitor compartment that is comprised of common myeloid progenitors (CMP), granulocyte-monocyte progenitors (GMP), and megakaryocyte-erythrocyte progenitors (MEP). However, analysis of the HSC and myeloid progenitor compartments showed a statistically significant decrease in the rate of apoptosis in both hematopoietic compartments, as assessed by staining with the 7-AAD viability dye and Annexin V (Figures 4A and 4B; ~2-fold for both HSC and myeloid progenitors; p = 0.005 and p = 0.04, respectively). Cell-cycle analysis of the HSC and myeloid progenitors using Hoechst 33342 and Pyro-

nin Y staining showed an increase in the percentage of G0/1 HSC and myeloid progenitor cells in G1 (Figures 4C and 4D), indicating increased exit out of quiescence and a trend toward an increased proportion of myeloid progenitor cells entering the S/G2/M phase of the cell cycle (33% versus 40% in wild-type and *RBP2*−/− mice, respectively; p < 0.07). Thus, there were quantitative differences in the HSC and myeloid progenitors of RBP2-deficient mice that were consistent with enhanced survival and increased cycling in these compartments. A more complete phenotypic description of the *RBP2*−/− mice will appear at a later date.

### Identification of RBP2-Responsive Genes

To begin to understand the molecular basis for these abnormalities and RBP2's role in transcriptional regulation, we performed mRNA profiling using DNA microarrays on proliferating *RBP2*+/+ and *RBP2*−/− MEFs grown under standard culture conditions (Tables 1 and S2). In replicate experiments the mRNAs encoding chemokine CXCL12/SDF1, c-Kit ligand, chemokine CXCL5, and chemokine CXCL1/Gro1 were increased in *RBP2*−/− cells relative to wild-type controls. At the same time, loss of RBP2 led
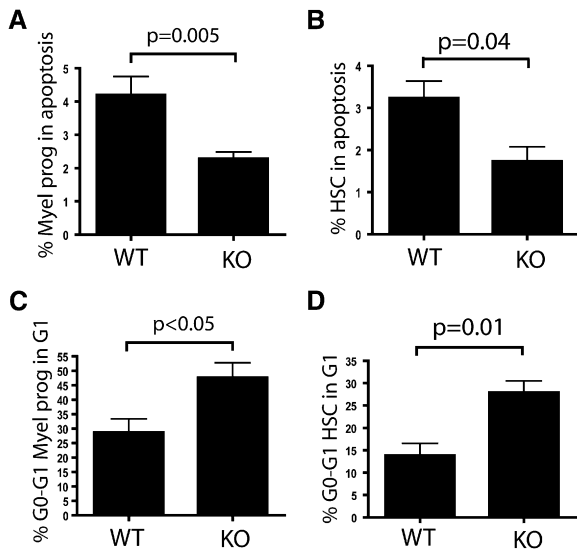
**Figure 4. RBP2 Knockout Mice Display Decreased Apoptosis and Increased Entry into G1 Phase of Cell Cycle in HSC and Myeloid Progenitor Compartments**

(A and B) Bone-marrow cells isolated from 23-week-old *RBP2* +/+ (WT) (n = 3) and *RBP2*−/− (KO) (n = 6) animals were stained for hematopoietic stem cell and progenitor markers, and apoptosis was assessed using 7-AAD and Annexin-V staining. *RBP2*-deficient HSC (LSK = Lin⁻ Sca-1⁺ c-kit⁺) and myeloid progenitors ("Myel prog") show decreased rates of apoptosis when compared to their wild-type littermates. Data are represented as mean ± standard error of the mean (SEM).

(C and D) Bone-marrow cells isolated from 23-week-old *RBP2* +/+ (WT) (n = 3) and *RBP2*−/− (KO) (n = 4) animals were stained for hematopoietic stem cell and progenitor markers, and the cell-cycle status was determined using Hoechst 33342 and Pyronin Y staining. *RBP2*-deficient HSC (LSK) and myeloid progenitors ("Myel prog") exhibit an increased entry into G1 phase (defined as % of G0-G1 cells in G1) of cell cycle when compared to their wild-type littermates. Data are represented as mean ± SEM.

to decreased levels of a handful of mRNAs, many of which encode proteins of unknown function.

We initially focused on *SDF1* because it was, quantitatively, the most RBP2-responsive mRNA amongst the cytokines mentioned above and because transgenic expression of *SDF1* in the mouse under the control of the Rous sarcoma virus promoter is sufficient to cause some of the hematological abnormalities we observed in *RBP2*−/− mice, including increased cell cycling and enhanced survival of myeloid progenitor cells (Broxmeyer et al., 2003a; Broxmeyer et al., 2003b). Increased expression of *SDF1* mRNA and protein by *RBP2*−/− relative to *RBP2*+/+ cells was confirmed by real-time RT-PCR and ELISA, respectively (Figures S1A and S1B). Moreover, RBP2 bound specifically to the *SDF1* promoter as determined by chromatin immunoprecipitation (ChIP) (Figures S1C; see also Figures 5A and 5B). Recovery of the *SDF1* promoter with the anti-RBP2 sera in these assays was, as expected, substantially reduced when these assays were performed with *RBP2*−/− MEFs (data not shown;

see also Figure 5B). Therefore *SDF1* appears to be a direct target of RBP2 mediated repression. *SDF1* expression was reproducibly increased in the muscle from *RBP2*−/− mice relative to wild-type mice (Figure S1D). In contrast, *SDF1* expression was not detectably increased in *RBP2*−/− brain, liver, bone marrow, and spleen (data not shown), suggesting that regulation of *SDF1* by RBP2 might be cell-type specific. Clearly additional studies will be needed to determine the relative contribution of *SDF1* to the phenotypic abnormalities noted above in *RBP2*−/− mice.

The availability of *RBP2*−/− mouse cells allowed us to also ask if RBP2, in addition to being sufficient (Figure 2), is also necessary for the demethylation of H3K4 in vivo. Immunoblot analysis using antibodies that recognize specific histone methylation marks, including an antibody specific for trimethylated H3K4, did not reveal any significant differences between wild-type and *RBP2*−/− MEFs (Figure S2A). Similar results were observed when *RBP2* was acutely inactivated in MEFs homozygous for the floxed *RBP2* allele (Figures 3A and S2B), suggesting that developmental plasticity does not account for the similarity between wild-type and *RBP2*−/− MEFs with respect to the total pool of methylated H3K4. However, decreased trimethylated H3K4, with a commensurate increased dimethylated H3K4, was detected on the *SDF1* promoter by ChIP in *RBP2*+/+ cells relative to *RBP2*−/− cells (Figures 5 and S3). This change was specific because H3K4 trimethylation was not altered in *SDF1* genomic fragments distant from the RBP2 binding site (Figure 5 and data not shown).

Finally, RBP2−/− cells were infected with retroviruses encoding wild-type RBP2 or RBP2-H483A. As expected, wild-type, but not mutant, RBP2 demethylated the *SDF1* promoter as determined by ChIP assay (Figure 6). Collectively, these results suggest that RBP2 is recruited to specific regions of the genome and is capable of acting as an H3K4 demethylase in vitro and in vivo.

## DISCUSSION

As is true for many transcription factors, RBP2 can act as a transcriptional activator or a transcriptional repressor in a context-dependent manner (Benevolenskaya et al., 2005; Chan and Hong, 2001). Demethylation of H3K4 likely contributes to RBP2's ability to repress transcription since trimethylated H3K4 is often associated with transcriptionally active genes. RBP2 also physically interacts with a complex that contains histone-deacetylase activity (Q.Y. and W.G.K., unpublished data), suggesting that transcriptional repression by RBP2 might also involve additional mechanisms. In support of this, the RBP2-H483A mutant significantly repressed *SDF1* expression when reintroduced into *RBP2*−/− mouse embryo fibroblasts (data not shown).

Furthermore, in light of the recent findings that histone demethylase activity of LSD1 is regulated by its associated factors (Lee et al., 2005; Shi et al., 2005; Yang

**Table 1. List of Genes Up- or Downregulated by 2-Fold or More in _RBP2_ −/− MEFs**

| Gene Name | Gene ID | Expression Level KO/WT | | |
| --- | --- | --- | --- | --- |
| | | Experiment 1 | Experiment 2 | Average |
| Cxcl12/Sdf1 | 20315 | 6.1 | 10.0 | 8.1 |
| Cxcl12/Sdf1 | 20315 | 5.8 | 7.1 | 6.4 |
| Cxcl5 | 20311 | 5.1 | 2.9 | 4 |
| Foxp2 | 114142 | 3.6 | 4.3 | 3.9 |
| Mtm1 | 17772 | 5.1 | 2.6 | 3.8 |
| Efemp1 | 216616 | 5.0 | 2.0 | 3.5 |
| Cxcl1/Gro1 | 14825 | 4.3 | 2.1 | 3.2 |
| H60 | 15101 | 2.5 | 3.8 | 3.1 |
| Ifi204 | 15951/672547 | 3.9 | 2.1 | 3 |
| Cdkn1b/p27 | 12576 | 3.3 | 2.6 | 2.9 |
| Nt5e | 23959 | 3.4 | 2.3 | 2.9 |
| Mgp | 17313 | 2.0 | 2.9 | 2.5 |
| BC049816 | 232313 | 3.1 | 1.7 | 2.4 |
| Dcn | 13179 | 3.1 | 1.7 | 2.4 |
| Kitl/SCF | 17311 | 2.7 | 1.9 | 2.3 |
| Aebp2 | 11569 | 2.3 | 2.2 | 2.3 |
| 2610044O15Rik | 72139 | 2.1 | 2.1 | 2.1 |
| Arhgdib | 11857 | 2.4 | 1.7 | 2.1 |
| Ppm2c | 381511 | 2.3 | 1.7 | 2 |
| Foxp1 | 108655 | −1.8 | −2.2 | −2 |
| Prdx2 | 21672 | −2.2 | −2.5 | −2.4 |
| Foxp1 | 108655 | −1.9 | −3.2 | −2.6 |
| Rbp2/Jarid1a | 214899 | −3.4 | −3.6 | −3.5 |
| Sorbs1 | 20411 | −3.7 | −4.7 | −4.2 |
| Sema4a | 20351 | −7.5 | −4.3 | −5.9 |
| Kcnd3 | 56543 | −17.4 | −2.5 | −10 |

et al., 2006), RBP2's histone-demethylase activity might also be modulated by associated protein factors in vivo. Such factors might, based on our work, influence whether RBP2 can recognize, and act upon, monomethylated H3K4 for example. Studies are currently underway to explore this possibility.

RBP2 contains both a canonical pRB binding motif, first identified in viral oncoproteins such as SV40 T, adenovirus E1A, and HPV E7, and a noncanonical pRB binding motif (Benevolenskaya et al., 2005; Defeo-Jones et al., 1991; Fattaey et al., 1993; Kim et al., 1994). pRB's ability to serve as a transcriptional coactivator, as well as its ability to promote differentiation, when reintroduced into _RB1_ −/− cells in vitro, are both tightly correlated with pRB's ability to bind to RBP2 (Benevolenskaya et al., 2005). Moreover, these pRB attributes can be phenocopied by downregulating RBP2 in _RB1_ −/− cells using siRNA (Benevolenskaya et al., 2005), suggesting that pRB and RBP2 antag-

onize one another and that pRB neutralizes RBP2 as a transcriptional repressor. On the other hand, RBP2 and pRB cooperate with one another to activate genes such as the bromodomain genes _Brd2_ and _Brd8_ (Benevolenskaya et al., 2005), suggesting that the functional interaction of pRB and RBP2 is actually more complex. It will be of interest to determine how and if binding to pRB alters RBP2 demethylase activity and whether pRB utilizes RBP2's demethylase activity in certain contexts to enforce changes in gene expression.

Based on their primary sequence similarity to RBP2, it is likely that all four JARID1 members act as H3K4 demethylases. Indeed, H3K4 demethylase activity has been observed for JARID1D (R. Shiekhattar, personal communication). JARID1B (PLU1), like RBP2, has been reported to act as a transcriptional repressor (Tan et al., 2003) . Preliminary results indicate it also possesses H3K4 demethylase activity (K. Y., R.J.K, and Y. Z., unpublished results).
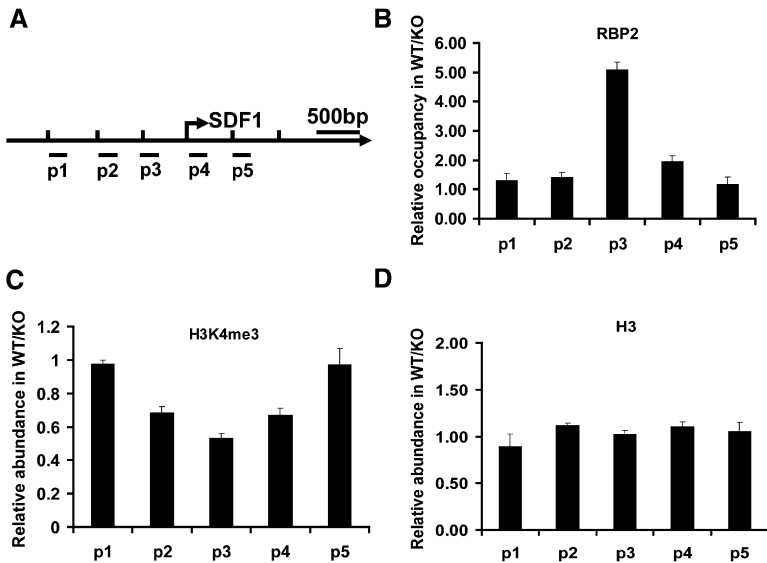
**Figure 5. RBP2 Binds to and Demethylates H3K4me3 at the *SDF1* Promoter**

(A) Schematic of the mouse *SDF1* genomic locus. The regions p1–p5 were analyzed by ChIP experiments.

(B–D) Relative abundance of RBP2 (B), H3K4me3 (C), and H3 (D) on the *SDF1* genomic regions, as determined by quantitative, real-time PCR analysis following ChIP of *RBP2* +/+ (WT) and *RBP2*−/− (KO) MEFs with the corresponding antibodies. Data are represented as mean ± SEM.

Interestingly, JARID1C (SMCX) and JARID1D (SMCY) map to the X and Y chromosome, respectively, raising the possibility that they play a role in establishing gender-specific gene-expression patterns. In fact, mutations in the JARID1C gene are associated with X-linked mental retardation (Jensen et al., 2005; Santos et al., 2006; Tzschach et al., 2006).

We did not observe global changes in H3K4 trimethylation when RBP2 was deleted from the mouse germline or acutely inactivated in MEFs in vitro, presumably due to redundancy with genes such as the other JARID1 family members mentioned above. It is also likely that redundancy is responsible for the viability of the *RBP2*−/− mice. Nonetheless, individual JARID1 family members are likely to have nonredundant roles in regulating certain cellular functions, as we observed hematological abnormalities in the *RBP2*−/− mice that correlated with derepression of RBP2 target cytokine genes such as *SDF1*. Further analysis of these mice should more clearly define

the contribution of *SDF1* in this setting and, more globally, to the nonredundant roles for RBP2 demethylase activity in vivo.

Interestingly, as a result of alternative splicing RBP2 contains either two or three PHD domains. The PHD domains of two other chromatin associated proteins, BPTF and ING2, have recently been shown to recognize trimethylated H3K4 (Li et al., 2006; Pena et al., 2006; Shi et al., 2006; Wysocka et al., 2006), indicating that the PHD domains may contribute to RBP2's ability to serve as a demethylase. It is intriguing that RBP2 has multiple PHD domains, however, and that the number of PHD domains is potentially regulated. Conceivably the multiple PHD domains bind independently, in cis, to appropriately modified H3 molecules and, as a result, ensure that RBP2 only recognizes adjacent methylated histones that have the proper spacing and orientation. It is also possible that this domain architecture contributes to the spacing with which RBP2 subsequently removes trimethylated
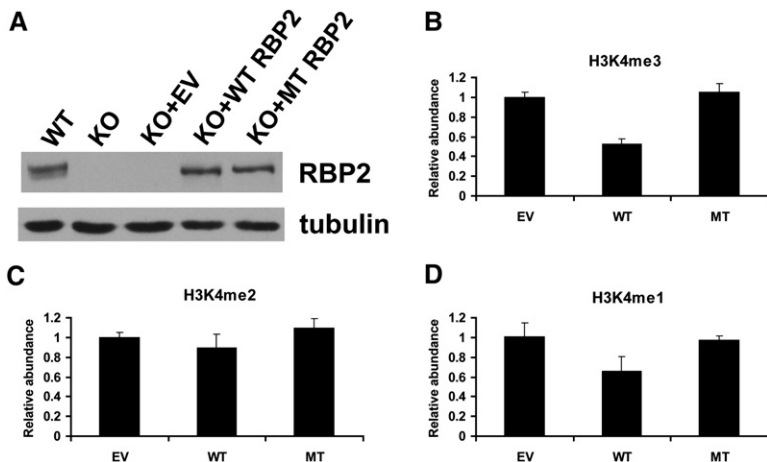


**Figure 6. Wild-Type RBP2, but Not JmjC Domain Mutant RBP2, Demethylates H3K4me3 at the *SDF1* Promoter**

(A) Immunoblot analysis of *RBP2*−/− (KO) MEFs that were stably infected with retroviruses expressing wild-type RBP2 (WT), RBP2-H483A (MT), or empty virus (EV). Uninfected *RBP2*+/+ (WT) MEFs were included as a control.

(B–D) Abundance of H3K4me3 (B), H3K4me2 (C), and H3K4me1 (D) on the p3 region of *SDF1*, as determined by quantitative, real-time PCR analysis following ChIP of *RBP2*−/− cells infected as in (A). Data are normalized to recovery using H3 antibody and are represented as mean ± SD.

H3K4 and/or contributes to its processivity. For example, the interaction of one PHD domain with trimethylated H3K4 might have to breathe in order for the previously bound trimethylated H3K4 to be acted upon by the adjacent JmjC domain. Once demethylated, RBP2 might slide along the chromatin until all of its PHD domains were again occupied by trimethylated H3K4.

2-oxoglutarate-dependent hydroxylases can be inhibited with drug-like small organic molecules (Epstein et al., 2001; Ivan et al., 2002; Lando et al., 2002). The growing list of histone demethylases that belong to this family raises the possibility that therapeutically advantageous changes in gene expression might, in time, be achieved by targeting specific demethylases with such compounds. In this regard, RBP2 conceivably contributes to the transformed phenotype in cancer cells that lack functional pRB and its paralog, PLU1, is overexpressed in breast cancer (Lu et al., 1999). It will be of interest to see whether genetic or pharmacological disruption of these family members affects tumor growth.

## EXPERIMENTAL PROCEDURES

### Constructs and Recombinant Protein

pcDNA3/HA-Flag-RBP2 was generated by inserting a Flag tag into the Cla I site of pcDNA3/HA-RBP2 (Benevolenskaya et al., 2005). pBABE-puro/HA-Flag-RBP2 was generated by inserting Flag-RBP2 cDNA into pBABE-puro/HA vector (Kondo et al., 2002). The H483A substitution mutation was introduced into pcDNA3/HA-Flag-RBP2 or pBABE-puro/HA-Flag-RBP2 by site-directed mutagenesis using the Quik-Change mutagenesis kit (Stratagene). For production of baculovirus-expressed protein, RBP2 was cloned into the Sal I and Xba I sites of a modified FastbacHTa (Invitrogen) vector engineered to contain an N-terminal Flag-tag. Generation of baculovirus that expresses Flag-RBP2 and purification of the recombinant protein from infected SF9 cells were performed as described previously (Cao and Zhang, 2004). Additional details are provided in the Supplemental Data.

### Antibodies

The RBP2 antibodies 1416 and 2471 were described previously (Benevolenskaya et al., 2005). The anti-RBP2 polyclonal antibody 2470 was raised in rabbits against glutathione S-transferase (GST)-RBP2 (1311–1358). Flag monoclonal M2 antibody and α-tubulin antibody (clone B-5-1-2) were from Sigma. H3K4me3 antibody (Ab8580), H3K4me1 antibody (Ab8895), H4K20me3 antibody (Ab9053), and H3 antibody (Ab1791) were from Abcam. H3K4me2 antibody (07-030), H3K9me2 antibody (05-768), and H4R3me2 antibody (07-213) were from Upstate. In some experiments, H3K4me2 antibody described previously (Feng et al., 2002) was used.

### Histone Demethylase Assays

Histone demethylase assays analyzing formaldehyde release were carried out using equal counts of labeled histone substrate and purified Flag-RBP2 as described previously (Tsukada et al., 2006), with the exception that a SET7 Y245A mutant was used to generate H3K4 substrate. Histone-demethylase assays using modified histone peptide substrates were carried out as described (Klose et al., 2006b) using peptides corresponding to amino acids 1–18 of histone H3 (Upstate 12-563[me1], Upstate 12-460[me2], and Upstate 12-564[me3]).

### Immunofluorescence

Indirect immunoflourscence was carried out using NIH3T3 cells grown in DMEM containing 10% fetal bovine serum (FBS) and penicillin/streptomycin. Cells grown on coverslips in 6-well plates were transfected with 2 μg of HA-Flag-RBP2 or HA-Flag-RBP2-H483A expression plasmid using FuGene 6 transfection reagent (Roche). Cells were fixed 24 hr posttransfection for 20 min in 4% paraformaldehyde, washed three times with PBS, and subsequently permeabilized for 20 min in 0.5% TritonX-100/PBS. Permeablized cells were washed two times in PBS and blocked in 3% BSA/PBS for 30 min. Cells were incubated with primary antibody in a humidified chamber for 1–3 hr using histone-modification antibodies at a dilution of 1:100–1:1000 and the Flag monoclonal M2 antibody (Sigma) at a dilution of 1:1000. After primary antibody incubation, cells were washed three times and incubated with FITC or Rhodamine conjugated secondary antibodies (Jackson ImmunoResearch Laboratories). Cells were washed twice with PBS, stained with 4,6-diamidino-2-phenylindole dihydrochloride (DAPI), and mounted on glass slides in fluorescent mounting medium (DAKO). Slides were analyzed on an AxioSkop fluorescent microscope (Zeiss).

### Construction of the Targeting Vector and Generation of *RBP2*-Deficient Mice

We isolated the RBP2 locus from RPCI-22 bacterial artificial chromosome library (Osoegawa et al., 2000). A conditional RBP2 targeting vector was generated by flanking RBP2 exons 5 and 6 with a 5′ *loxP* site and a 3′ *Frt*-PGK-neomycin-*Frt-LoxP* expression cassette (Bardeesy et al., 2002). After electroporation of 129/SvEv embryonic stem (ES) cells and selection at 200 μg/ml G418, we screened 192 ES cell clones by PCR and Southern blot analysis and identified 11 correct recombinants at the RBP2 locus. Two of the correctly targeted ES clones were injected into C57BL/6 blastocysts, and chimeric mice were bred into C57BL/6. Germline transmitting mice were bred to CAGG-*Flpe* (Rodriguez et al., 2000) and EIIa-*Cre* (Lakso et al., 1996) transgenic mice to generate the lox and null alleles, respectively. *Cre*+RBP2+/− and *Flpe*+RBP2+/lox mice were backcrossed once or twice to C57BL/6, and progeny of these crosses that were *Cre*− and *Flpe*− were then used to generate the experimental cohort. The genotypes of the mice were determined by multiplex PCR, Southern blot analysis, or by Quantitative PCR (Transnetyx). Primers used for multiplex PCR in genotyping analysis are available in the Supplemental Data. All mice were maintained in the research animal facility of the Dana-Farber Cancer Institute in accordance with the NIH guidelines, and all procedures involving mice were approved by the Dana-Farber Cancer Institute IACUC.

### Cell Culture

MEFs were isolated from 13.5 days postcoitum (dpc) embryos using standard procedures. MEFs were maintained in Dulbecco's modified Eagle's medium (DMEM) containing 10% FBS (Hyclone). Phoenix packaging cells (a generous gift of Dr. Gary Nolan, Department of Molecular Pharmacology, Stanford University, CA) cells were grown in DMEM containing 10% FBS. Retroviral plasmids were transfected into the Phoenix cells using FuGene 6 reagent (Roche Molecular Biochemicals) according to the manufacturer's instructions. Tissue-culture supernatant containing retroviruses was harvested 48 hr later, passed though a 0.45 μm filter, and added to cells in the presence of 4 μg/ml polybrene. Immortalized MEFs were generated by stably infecting the primary MEFs with retroviruses encoding the K1 mutant of the SV40 large T antigen, which inactivates p53 pathway, but not pRB pathway (Quartin et al., 1994). To acutely inactivate RBP2, immortalized *RBP2*+/lox or *RBP2*lox/lox MEFs were infected with retroviruses encoding Cre recombinase. To reintroduce RBP2 into the immortalized *RBP2*−/− MEFs, cells were stably infected with retroviruses encoding wild-type RBP2 or RBP2-H483A mutant and maintained in media containing 3 μg/ml puromycin.

### Western Blot Analysis and ELISA

See the Supplemental Data.

### Real-Time RT-PCR

Total RNA was isolated using RNeasy mini kit with on-column DNase digestion (Qiagen). First-strand cDNA was generated using Strata-Script First-Stand Synthesis System (Statagene). Real-time PCR was performed in triplicate using QuantiTect SYBR Green PCR master mix (Qiagen) and the Mx3000P QPCR system (Stratagene). Primers are described in the Supplemental Data. All values were normalized to the level of GAPDH mRNA abundance.

### Cell Staining and FACS Analysis

For multiparameter flow cytometry, bone-marrow mononuclear cells were flushed from hind-leg bones with RPMI (Cambrex, Biowhittaker) containing 10% FBS (Gibco) and penicillin/streptomycin (Cambrex, Biowhittaker), incubated on ice with red blood cell lysis solution (Puregene) and washed in PBS (Gibco) containing 2% FBS. LSK, CMP, GMP, MEP, and CLP populations were analyzed using a FACSAria instrument (Becton Dickinson, Mountain View, CA) as previously reported (Akashi et al., 2000; Kondo et al., 1997). Apoptosis was determined by staining freshly harvested bone-marrow mononuclear cells with lineage, stem, and progenitor markers, followed by Annexin-V and 7-AAD staining. Cell-cycle analysis was carried out as previously reported (Cheng et al., 2000). Additional analyses were carried out on a 4-color FACSCalibur cytometer (Becton Dickinson, Mountain View, CA) using samples that were washed with PBS and 0.1% bovine serum albumin (BSA) (Sigma), blocked with Fc-block (BD-Pharmingen) for 10 min, and stained with the following monoclonal antibodies in PBS + 0.1% BSA for 30 min: B220-APC, Mac-1-FITC, Gr-1-APC, and 7-AAD. A minimum of 10,000 events was acquired and analyzed using CellQuest software.

### Gene-Expression Profiling

Subconfluent wild-type and *RBP2*−/− primary MEFs at passage 3 were harvested for RNA isolation using RNeasy mini kit with on-column DNase digestion (Qiagen). Gene-expression profiling was performed using the Affymetrix M430 2.0 chip. Analysis of the raw gene expression profiling was performed using dChip software (Li and Hung Wong, 2001). mRNA expression levels in *RBP2*−/− MEFs were compared to wild-type MEFs. The genes listed were selected if they were up- or downregulated 1.5-fold in each of the duplicate experiments and up- or downregulated by 2-fold or more on average in *RBP2*−/− MEFs. The gene-expression profiling data can be found in the Gene Expression Omnibus (GEO) of NCBI at http://www.ncbi.nlm.nih.gov/geo/ through accession number GSE6945.

### ChIP

Subconfluent *RBP2*+/+ and *RBP2*−/− MEFs grown in 150 mm dishes were first treated with DMEM containing 1% formaldehyde for 15 min. The crosslinking was stopped by the addition of 0.125 M glycine for 5 min. After washing twice with PBS, the cells were resuspended in 1 ml of lysis buffer A (10 mM Tris HCl (pH 7.5), 10 mM KCl, 5 mM MgCl$_2$, 0.5% NP40) with 1 mM PMSF and incubated on ice for 10 min. After centrifugation at 2000 rpm for 5 min, the cell pellets were resuspended in SDS lysis buffer (50 mM Tris HCl (pH 7.9), 10 mM EDTA, 0.5% SDS) supplemented with completer protease inhibitor cocktail (Roche Molecular Biochemicals). The chromatin samples were then sonicated into fragments with an average length of 1 kb. After centrifugation at 13,000 rpm for 10 min, the supernatants were diluted 1:4 with ChIP dilution buffer (12.5 mM Tris HCl [pH 7.9], 187.5 mM NaCl, 1.25% Triton X-100) containing protease inhibitors. ChIP assays were then performed with the indicated antibodies. PCR analyses were then performed to determine the amount of targets in the ChIP samples. In some cases, quantitative, real-time PCR was performed in triplicate using QuantiTect SYBR Green PCR master mix (Qiagen) and the Mx3000P QPCR system (Stratagene). Primers are described in the Supplemental Data. The relative amount of immunoprecipitated DNA to input DNA or immunoprecipitated DNA by histone H3 antibody was plotted in the figures.

### Supplemental Data

Supplemental Data include Supplemental Experimental Procedures, Supplemental References, three figures, and two tables and can be found with this article online at http://www.cell.com/cgi/content/full/128/5/889/DC1/.

### REFERENCES

Akashi, K., Traver, D., Miyamoto, T., and Weissman, I.L. (2000). A clonogenic common myeloid progenitor that gives rise to all myeloid lineages. Nature *404*, 193–197.

Bannister, A.J., Zegerman, P., Partridge, J.F., Miska, E.A., Thomas, J.O., Allshire, R.C., and Kouzarides, T. (2001). Selective recognition of methylated lysine 9 on histone H3 by the HP1 chromo domain. Nature *410*, 120–124.

Bardeesy, N., Sinha, M., Hezel, A.F., Signoretti, S., Hathaway, N.A., Sharpless, N.E., Loda, M., Carrasco, D.R., and DePinho, R.A. (2002). Loss of the Lkb1 tumour suppressor provokes intestinal polyposis but resistance to transformation. Nature *419*, 162–167.

Benevolenskaya, E.V., Murray, H.L., Branton, P., Young, R.A., and Kaelin, W.G., Jr. (2005). Binding of pRB to the PHD protein RBP2 promotes cellular differentiation. Mol. Cell *18*, 623–635.

Broxmeyer, H.E., Cooper, S., Kohli, L., Hangoc, G., Lee, Y., Mantel, C., Clapp, D.W., and Kim, C.H. (2003a). Transgenic expression of stromal cell-derived factor-1/CXC chemokine ligand 12 enhances myeloid progenitor cell survival/antiapoptosis in vitro in response to growth factor withdrawal and enhances myelopoiesis in vivo. J. Immunol. *170*, 421–429.

Broxmeyer, H.E., Kohli, L., Kim, C.H., Lee, Y., Mantel, C., Cooper, S., Hangoc, G., Shaheen, M., Li, X., and Clapp, D.W. (2003b). Stromal cell-derived factor-1/CXCL12 directly enhances survival/antiapoptosis of myeloid progenitor cells through CXCR4 and G(alpha)i proteins and enhances engraftment of competitive, repopulating stem cells. J. Leukoc. Biol. *73*, 630–638.

Cao, R., and Zhang, Y. (2004). SUZ12 is required for both the histone methyltransferase activity and the silencing function of the EED-EZH2 complex. Mol. Cell *15*, 57–67.

Chan, S.W., and Hong, W. (2001). Retinoblastoma-binding protein 2 (Rbp2) potentiates nuclear hormone receptor-mediated transcription. J. Biol. Chem. *276*, 28402–28412.

Cheng, T., Rodrigues, N., Shen, H., Yang, Y., Dombkowski, D., Sykes, M., and Scadden, D.T. (2000). Hematopoietic stem cell quiescence maintained by p21cip1/waf1. Science *287*, 1804–1808.

Cloos, P.A., Christensen, J., Agger, K., Maiolica, A., Rappsilber, J., Antal, T., Hansen, K.H., and Helin, K. (2006). The putative oncogene GASC1 demethylates tri- and dimethylated lysine 9 on histone H3. Nature *442*, 307–311.

Defeo-Jones, D., Huang, P.S., Jones, R.E., Haskell, K.M., Vuocolo, G.A., Hanobik, M.G., Huber, H.E., and Oliff, A. (1991). Cloning of cDNAs for cellular proteins that bind to the retinoblastoma gene product. Nature *352*, 251–254.

Epstein, A.C., Gleadle, J.M., McNeill, L.A., Hewitson, K.S., O'Rourke, J., Mole, D.R., Mukherji, M., Metzen, E., Wilson, M.I., Dhanda, A., et al. (2001). C. elegans EGL-9 and mammalian homologs define a family of dioxygenases that regulate HIF by prolyl hydroxylation. Cell *107*, 43–54.

Falnes, P.O., Johansen, R.F., and Seeberg, E. (2002). AlkB-mediated oxidative demethylation reverses DNA damage in Escherichia coli. Nature *419*, 178–182.

Fattaey, A.R., Helin, K., Dembski, M.S., Dyson, N., Harlow, E., Vuocolo, G.A., Hanobik, M.G., Haskell, K.M., Oliff, A., Defeo-Jones, D., et al. (1993). Characterization of the retinoblastoma binding proteins RBP1 and RBP2. Oncogene *8*, 3149–3156.

Feng, Q., Wang, H., Ng, H.H., Erdjument-Bromage, H., Tempst, P., Struhl, K., and Zhang, Y. (2002). Methylation of H3-lysine 79 is mediated by a new family of HMTases without a SET domain. Curr. Biol. *12*, 1052–1058.

Fischle, W., Wang, Y., Jacobs, S.A., Kim, Y., Allis, C.D., and Khorasanizadeh, S. (2003). Molecular basis for the discrimination of repressive methyl-lysine marks in histone H3 by Polycomb and HP1 chromodomains. Genes Dev. *17*, 1870–1881.

Fodor, B.D., Kubicek, S., Yonezawa, M., O'Sullivan, R.J., Sengupta, R., Perez-Burgos, L., Opravil, S., Mechtler, K., Schotta, G., and Jenuwein, T. (2006). Jmjd2b antagonizes H3K9 trimethylation at pericentric heterochromatin in mammalian cells. Genes Dev. *20*, 1557–1562.

Gildea, J.J., Lopez, R., and Shearn, A. (2000). A screen for new trithorax group genes identified little imaginal discs, the Drosophila melanogaster homologue of human retinoblastoma binding protein 2. Genetics *156*, 645–663.

Huang, Y., Fang, J., Bedford, M.T., Zhang, Y., and Xu, R.M. (2006). Recognition of histone H3 lysine-4 methylation by the double tudor domain of JMJD2A. Science *312*, 748–751.

Huyen, Y., Zgheib, O., Ditullio, R.A., Jr., Gorgoulis, V.G., Zacharatos, P., Petty, T.J., Sheston, E.A., Mellert, H.S., Stavridi, E.S., and Halazonetis, T.D. (2004). Methylated lysine 79 of histone H3 targets 53BP1 to DNA double-strand breaks. Nature *432*, 406–411.

Ivan, M., Haberberger, T., Gervasi, D.C., Michelson, K.S., Gunzler, V., Kondo, K., Yang, H., Sorokina, I., Conaway, R.C., Conaway, J.W., et al. (2002). Biochemical purification and pharmacological inhibition of a mammalian prolyl hydroxylase acting on hypoxia-inducible factor. Proc. Natl. Acad. Sci. USA *99*, 13459–13464.

Jensen, L.R., Amende, M., Gurok, U., Moser, B., Gimmel, V., Tzschach, A., Janecke, A.R., Tariverdian, G., Chelly, J., Fryns, J.P., et al. (2005). Mutations in the JARID1C gene, which is involved in transcriptional regulation and chromatin remodeling, cause X-linked mental retardation. Am. J. Hum. Genet. *76*, 227–236.

Kim, Y.W., Otterson, G.A., Kratzke, R.A., Coxon, A.B., and Kaye, F.J. (1994). Differential specificity for binding of retinoblastoma binding protein 2 to RB, p107, and TATA-binding protein. Mol. Cell. Biol. *14*, 7256–7264.

Klose, R.J., Kallin, E.M., and Zhang, Y. (2006a). JmjC-domain-containing proteins and histone demethylation. Nat. Rev. Genet. *7*, 715–727.

Klose, R.J., Yamane, K., Bae, Y., Zhang, D., Erdjument-Bromage, H., Tempst, P., Wong, J., and Zhang, Y. (2006b). The transcriptional repressor JHDM3A demethylates trimethyl histone H3 lysine 9 and lysine 36. Nature *442*, 312–316.

Kondo, K., Klco, J., Nakamura, E., Lechpammer, M., and Kaelin, W.G., Jr. (2002). Inhibition of HIF is necessary for tumor suppression by the von Hippel-Lindau protein. Cancer Cell *1*, 237–246.

Kondo, M., Weissman, I.L., and Akashi, K. (1997). Identification of clonogenic common lymphoid progenitors in mouse bone marrow. Cell *91*, 661–672.

Kortschak, R.D., Tucker, P.W., and Saint, R. (2000). ARID proteins come in from the desert. Trends Biochem. Sci. *25*, 294–299.

Lachner, M., O'Carroll, D., Rea, S., Mechtler, K., and Jenuwein, T. (2001). Methylation of histone H3 lysine 9 creates a binding site for HP1 proteins. Nature *410*, 116–120.

Lakso, M., Pichel, J.G., Gorman, J.R., Sauer, B., Okamoto, Y., Lee, E., Alt, F.W., and Westphal, H. (1996). Efficient in vivo manipulation of mouse genomic sequences at the zygote stage. Proc. Natl. Acad. Sci. USA *93*, 5860–5865.

Lando, D., Peet, D.J., Whelan, D.A., Gorman, J.J., and Whitelaw, M.L. (2002). Asparagine hydroxylation of the HIF transactivation domain a hypoxic switch. Science *295*, 858–861.

Lee, M.G., Wynder, C., Cooch, N., and Shiekhattar, R. (2005). An essential role for CoREST in nucleosomal histone 3 lysine 4 demethylation. Nature *437*, 432–435.

Li, C., and Hung Wong, W. (2001). Model-based analysis of oligonucleotide arrays: model validation, design issues and standard error application. Genome Biol. *2*, RESEARCH0032.

Li, H., Ilin, S., Wang, W., Duncan, E.M., Wysocka, J., Allis, C.D., and Patel, D.J. (2006). Molecular basis for site-specific read-out of histone H3K4me3 by the BPTF PHD finger of NURF. Nature *442*, 91–95.

Lu, P.J., Sundquist, K., Baeckstrom, D., Poulsom, R., Hanby, A., Meier-Ewert, S., Jones, T., Mitchell, M., Pitha-Rowe, P., Freemont, P., et al. (1999). A novel gene (PLU-1) containing highly conserved putative DNA/chromatin binding motifs is specifically up-regulated in breast cancer. J. Biol. Chem. *274*, 15633–15645.

Martin, C., and Zhang, Y. (2005). The diverse functions of histone lysine methylation. Nat. Rev. Mol. Cell Biol. *6*, 838–849.

Metzger, E., Wissmann, M., Yin, N., Muller, J.M., Schneider, R., Peters, A.H., Gunther, T., Buettner, R., and Schule, R. (2005). LSD1 demethylates repressive histone marks to promote androgen-receptor-dependent transcription. Nature *437*, 436–439.

Min, J., Zhang, Y., and Xu, R.M. (2003). Structural basis for specific binding of Polycomb chromodomain to histone H3 methylated at Lys 27. Genes Dev. *17*, 1823–1828.

Osoegawa, K., Tateno, M., Woon, P.Y., Frengen, E., Mammoser, A.G., Catanese, J.J., Hayashizaki, Y., and de Jong, P.J. (2000). Bacterial artificial chromosome libraries for mouse sequencing and functional analysis. Genome Res. *10*, 116–128.

Pena, P.V., Davrazou, F., Shi, X., Walter, K.L., Verkhusha, V.V., Gozani, O., Zhao, R., and Kutateladze, T.G. (2006). Molecular mechanism of histone H3K4me3 recognition by plant homeodomain of ING2. Nature *442*, 100–103.

Pray-Grant, M.G., Daniel, J.A., Schieltz, D., Yates, J.R., 3rd, and Grant, P.A. (2005). Chd1 chromodomain links histone H3 methylation with SAGA- and SLIK-dependent acetylation. Nature *433*, 434–438.

Quartin, R.S., Cole, C.N., Pipas, J.M., and Levine, A.J. (1994). The amino-terminal functions of the simian virus 40 large T antigen are required to overcome wild-type p53-mediated growth arrest of cells. J. Virol. *68*, 1334–1341.

Rodriguez, C.I., Buchholz, F., Galloway, J., Sequerra, R., Kasper, J., Ayala, R., Stewart, A.F., and Dymecki, S.M. (2000). High-efficiency deleter mice show that FLPe is an alternative to Cre-loxP. Nat. Genet. *25*, 139–140.

Sanders, S.L., Portoso, M., Mata, J., Bahler, J., Allshire, R.C., and Kouzarides, T. (2004). Methylation of histone H4 lysine 20 controls recruitment of Crb2 to sites of DNA damage. Cell *119*, 603–614.

Santos, C., Rodriguez-Revenga, L., Madrigal, I., Badenas, C., Pineda, M., and Mila, M. (2006). A novel mutation in JARID1C gene associated with mental retardation. Eur. J. Hum. Genet. *14*, 583–586.

Shi, X., Hong, T., Walter, K.L., Ewalt, M., Michishita, E., Hung, T., Carney, D., Pena, P., Lan, F., Kaadige, M.R., et al. (2006). ING2 PHD domain links histone H3 lysine 4 methylation to active gene repression. Nature *442*, 96–99.

Shi, Y., Lan, F., Matson, C., Mulligan, P., Whetstine, J.R., Cole, P.A., Casero, R.A., and Shi, Y. (2004). Histone demethylation mediated by the nuclear amine oxidase homolog LSD1. Cell *119*, 941–953.

Shi, Y.J., Matson, C., Lan, F., Iwase, S., Baba, T., and Shi, Y. (2005). Regulation of LSD1 histone demethylase activity by its associated factors. Mol. Cell *19*, 857–864.

Shilatifard, A. (2006). Chromatin modifications by methylation and ubiquitination: implications in the regulation of gene expression. Annu. Rev. Biochem. *75*, 243–269.

Tan, K., Shaw, A.L., Madsen, B., Jensen, K., Taylor-Papadimitriou, J., and Freemont, P.S. (2003). Human PLU-1 Has transcriptional repression properties and interacts with the developmental transcription factors BF-1 and PAX9. J. Biol. Chem. *278*, 20507–20513.

Trewick, S.C., Henshaw, T.F., Hausinger, R.P., Lindahl, T., and Sedgwick, B. (2002). Oxidative demethylation by Escherichia coli AlkB directly reverts DNA base damage. Nature *419*, 174–178.

Trewick, S.C., McLaughlin, P.J., and Allshire, R.C. (2005). Methylation: lost in hydroxylation? EMBO Rep. *6*, 315–320.

Tsukada, Y., Fang, J., Erdjument-Bromage, H., Warren, M.E., Borchers, C.H., Tempst, P., and Zhang, Y. (2006). Histone demethylation by a family of JmjC domain-containing proteins. Nature *439*, 811–816.

Tzschach, A., Lenzner, S., Moser, B., Reinhardt, R., Chelly, J., Fryns, J.P., Kleefstra, T., Raynaud, M., Turner, G., Ropers, H.H., et al. (2006). Novel JARID1C/SMCX mutations in patients with X-linked mental retardation. Hum. Mutat. *27*, 389.

Whetstine, J.R., Nottke, A., Lan, F., Huarte, M., Smolikov, S., Chen, Z., Spooner, E., Li, E., Zhang, G., Colaiacovo, M., et al. (2006). Reversal of histone lysine trimethylation by the JMJD2 family of histone demethylases. Cell *125*, 467–481.

Wilsker, D., Probst, L., Wain, H.M., Maltais, L., Tucker, P.W., and Moran, E. (2005). Nomenclature of the ARID family of DNA-binding proteins. Genomics *86*, 242–251.

Wysocka, J., Swigut, T., Milne, T.A., Dou, Y., Zhang, X., Burlingame, A.L., Roeder, R.G., Brivanlou, A.H., and Allis, C.D. (2005). WDR5 associates with histone H3 methylated at K4 and is essential for H3 K4 methylation and vertebrate development. Cell *121*, 859–872.

Wysocka, J., Swigut, T., Xiao, H., Milne, T.A., Kwon, S.Y., Landry, J., Kauer, M., Tackett, A.J., Chait, B.T., Badenhorst, P., et al. (2006). A PHD finger of NURF couples histone H3 lysine 4 trimethylation with chromatin remodelling. Nature *442*, 86–90.

Yamane, K., Toumazou, C., Tsukada, Y., Erdjument-Bromage, H., Tempst, P., Wong, J., and Zhang, Y. (2006). JHDM2A, a JmjC-containing H3K9 demethylase, facilitates transcription activation by androgen receptor. Cell *125*, 483–495.

Yang, M., Gocke, C.B., Luo, X., Borek, D., Tomchick, D.R., Machius, M., Otwinowski, Z., and Yu, H. (2006). Structural basis for CoREST-dependent demethylation of nucleosomes by the human LSD1 histone demethylase. Mol. Cell *23*, 377–387.